Experimental Techniques (2023) 47:1275–1283
https://doi.org/10.1007/s40799-022-00613-1

APPLICATIONS PAPER

Evaluating The Characteristics of Thin-Walled S235 Steel Under Three-Point Bending with Different Loading Parameters

A. Ünlü[1] · E. Esener[1]

Received: 7 June 2022 / Accepted: 14 September 2022 / Published online: 8 November 2022

Abstract

In real collision conditions, axial crushing rarely occurs. Generally, lateral collapse occurs in thin-walled beams under collision conditions. The bending displacement of thin-walled beams is one of the most important deformation mechanisms to dissipate the kinetic energy generated by the collision. Bending displacement deformation occurs in pure bending and three-point bending modes. However, pure bending is rarely encountered in real collision events. The three-point bending analysis is more complex as it involves variable bending moment and shear forces at different cross-sections. In this study, it is aimed to investigate the behavior of thin-walled s235 structural steel under three-point bending in three different section geometries as square, rectangular and, tube. Experiments were performed using three different punch geometries and three different span distances for each section. It is concluded that the influence of section geometries of thin-walled structures, span distance, and punch radius has a significant effect on the deformation pattern and force/bending moment response of thin-walled structures.

Keywords Bending behavior · thin-walled · structural steel · energy absorption

Introduction

Today, thin-walled structures are widely used as energy-absorbing structural components in many industries such as automobiles, trains, offshore structures, construction, military equipment, etc. [1]. The energy absorption efficiency and collision resistance of thin-walled elements in various engineering applications have been investigated by many methods such as analytical [2], numerical [3, 4], experimental [5–7], and design optimization [8–10].

Today, the mobile vehicle industry is one of the sectors where research and development activities of thin-walled elements used as energy-absorbing structural components are carried out intensively. Axial crushing of thin-walled elements used as energy-absorbing structural components in the mobile vehicle industry has been investigated in many different applications [11]. However, in real collision conditions, axial crushing rarely occurs. Generally, lateral collapse occurs in thin-walled beams under collision conditions. The bending displacement of thin-walled beams is one of the most important deformation mechanisms to dissipate the kinetic energy generated by the collision and ensure the safety of passengers or cargo [12]. During a collision, the hollow buffer beams enter a localized bending displacement mode [13]. Bending displacement deformation occurs in pure bending and three-point bending modes. Pure bending is relatively easy to analyze compared to three-point bending. However, pure bending is rarely encountered in real collision events. The three-point bending analysis is more complex as it involves variable bending moment and shear forces at different cross-Sect. [14]. Therefore, examining and improving the three-point bending behavior of thin-walled structures is of great importance for engineering.

In this context, different approaches are used in various engineering applications to improve the bending behavior of thin-walled beams, to improve the collision resistance performance of the elements, and to increase their energy absorption capacity at the same time. One of these approaches; is to transform thin-walled elements into multicellular tubes. In a study on this subject, Zhang et al. [11] investigated the three-point bending behavior of hollow tubes, EMC (embedded multi-cell) tubes, and TMC (traditional

✉ E. Esener
emre.esener@bilecik.edu.tr

[1] Mechanical Engineering Department, Bilecik Seyh Edebali University, Bilecik, Turkey

multi-cell) tubes. EMC tubes were found to show a much higher average breaking force and SEA value compared to hollow tubes. However, TMC tubes also showed excellent performance under three-point bending. Another effective approach that can be used instead of making thin-walled elements multicellular is to add filler. Thus, it is possible to increase the load-carrying capacity and energy absorption efficiency of thin-walled structures. Generally, foam padding [3], tube padding [15], circular or square pipe padding [16], concrete padding [17], and honeycomb padding [18] to increase energy absorption efficiency in energy-absorbing structures are used. Among these fillings, the most widely used foam filling material in the literature is aluminum foam [19, 20]. In a study conducted in this context; Fang et al. [21] concluded that aluminum foam infill can significantly alter the bending behavior in terms of energy absorption and deformation patterns. Filling the thin-walled elements with foam increases the energy absorption efficiency while also providing a significant weight gain. However, it is possible to increase the structural strength of the elements while providing lightness without adding a filler. Steel [22–26] and aluminum alloys [19–21, 27] have been widely used in the production of thin-walled elements to date. In a study conducted with this approach; Zhu et al. [28] investigated the three-point bending behavior of CFRP (Carbon fiber reinforced plastic) composite material and conducted optimization studies. They showed that the optimized CFRP buffer beam meets all the requirements for crash resistance with a maximum weight reduction of up to 51.7% compared to a high-strength steel buffer beam. In addition to the material, the influence of section geometry is inevitable in the three-point bending behavior of thin-walled elements. Thin-walled elements are produced in many shapes such as circular [10], rectangular [14], square [15], hat Sect. [29], and sandwich [30]. However, in many studies examined, it is seen that uniform geometry is used, in other words, the effect of geometry on thin-walled elements is not clearly shown [8, 22–24, 27]. In this context, suitable results can be obtained by optimizing hollow-single-cell tubes with loading parameters. For example, in a study conducted in this context; Huang et al. [31] studied the bending behavior of thin-walled aluminum square-hollow tubes and examined the effect of loading parameters. They found that the average crushing force of thin-walled square tubes could be increased up to 78%. Thus, it has been observed that hollow tube materials can give appropriate results with optimized loading parameters, without an additional process, additional weight (fill, cell, etc.), time, and cost loss. In the production of these structural elements, carbon steels have great importance thanks to their tensile strength, yield limits, and construction strengths. Among these steels, s235 steels, which are called structural steels, come to the fore with their sufficient strength, impact resistance, toughness, cost, and availability advantages [32, 33].

In this study, the behavior of thin-walled s235 structural steel under three-point bending was investigated in

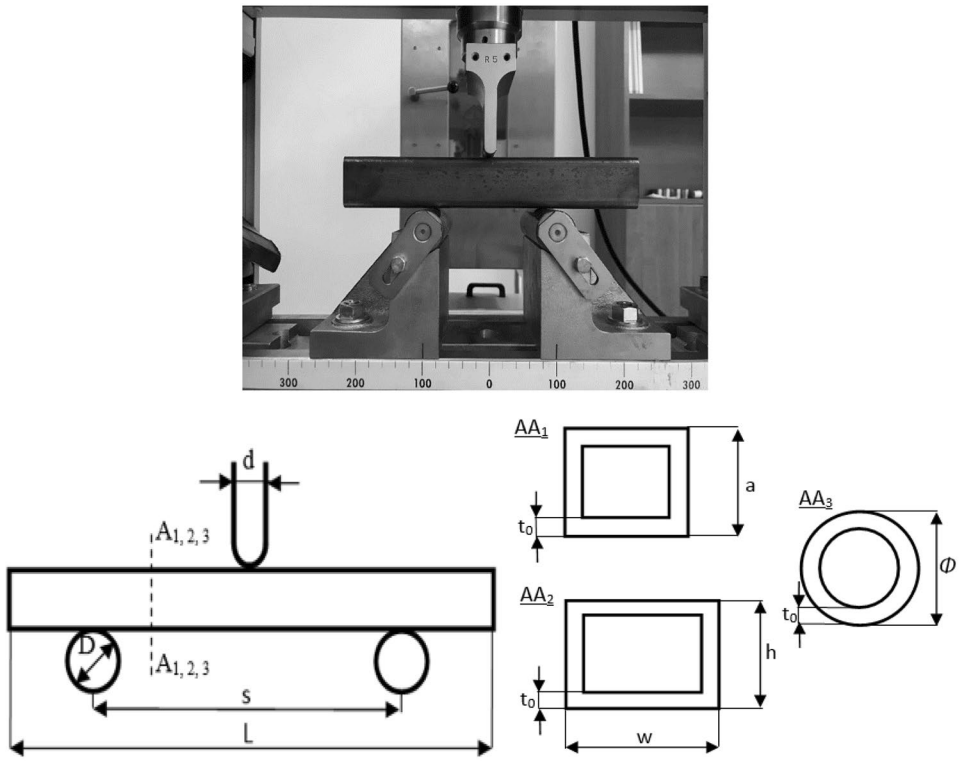

Fig. 1 Sample geometries and experimental setup of three-point bending test

Table 1 Dimensions of sample sections and loading parameters

Section	h	w	t_0	Φ	a
AA_1(Square)	-	-	2	-	40.3
AA_2(Rectangular)	30	40	1.75	-	-
AA_3(Tube)	-	-	1.95	40.3	-
Loading Parameters					
D	**L**	**s**		**d**	
30	250	100		10	
		160		20	
		200		30	

* All dimensions are in mm

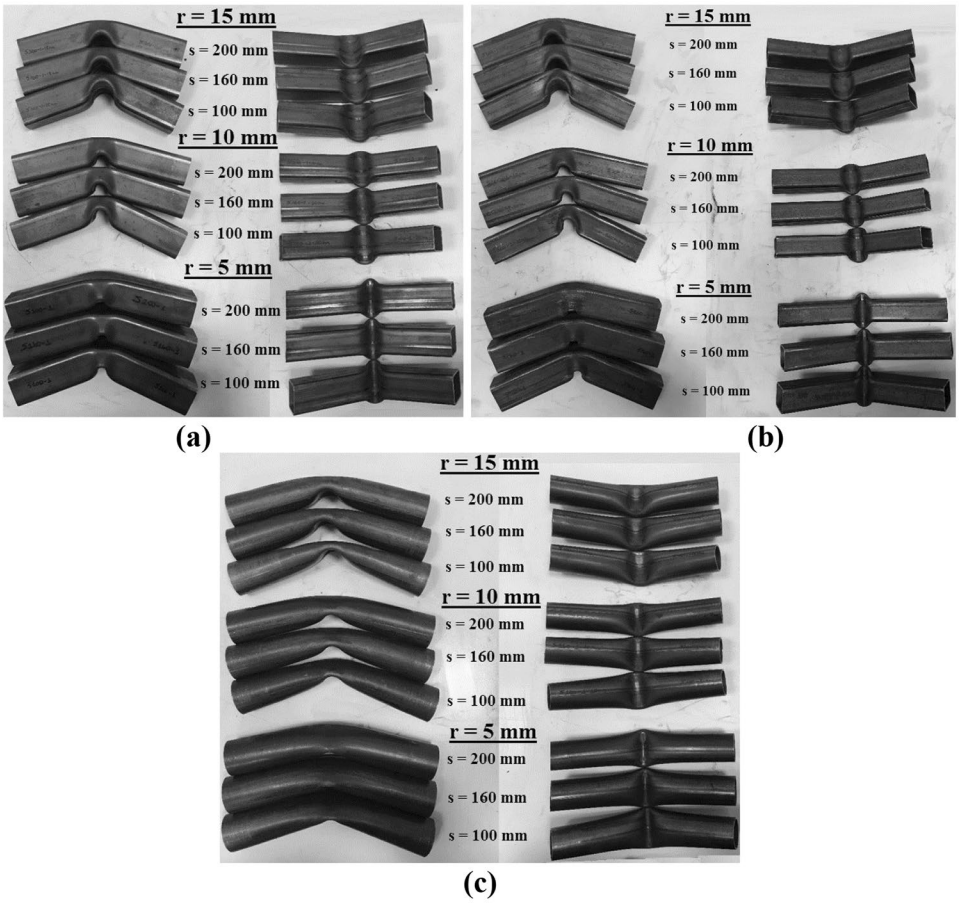

Fig. 2 Sample forms after experiments **(a)** Square section **(b)** Rectangular section **(c)** Tube section

three different section geometries as square, rectangular and, tube. Experiments were performed using three different punch geometries and three different span distances for each section. As a result of the study, the behavior of s235 steel under three-point bending under different loading conditions has been revealed.

Material and Method

In this study, three-point bending tests were carried out for s235 steel using different loading parameters. Section geometry, span distance, and punch radius were used as loading parameters. Experimental studies were evaluated in terms of force-stroke curves and energy absorption. The experimental tools used in the study, the schematic representation of the experimental set, and the sample section geometries are shown in Fig. 1. The geometric dimensions in Fig. 1 are given in Table 1.

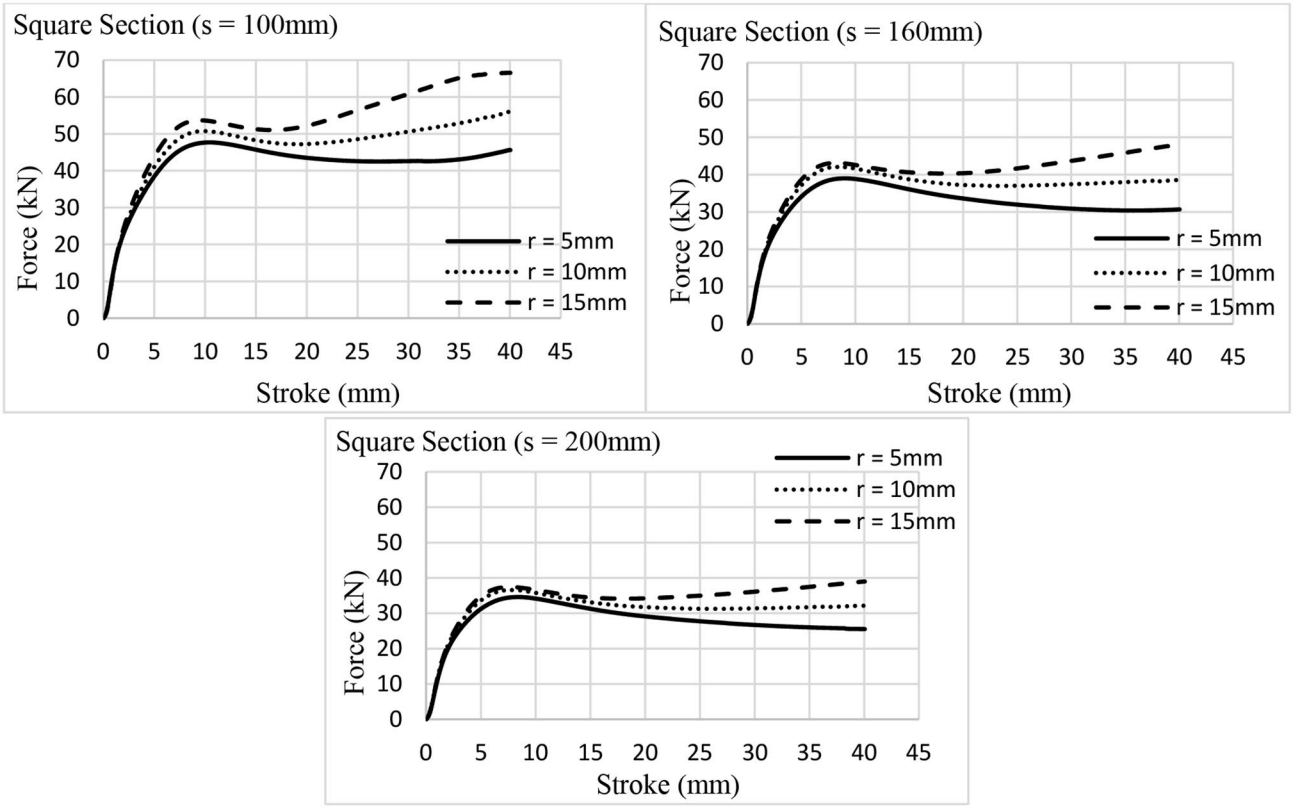

Fig. 3 Force-Stroke curves for square section with different punch radius

As can be seen in Fig. 1, three different profile sections were studied within the scope of the study (square, rectangular, and tube). Three-point bending tests were carried out at three different punch radii, 5, 10, and 15 mm, for three different cross-section profiles. All experimental studies were carried out in three different span distances of 100, 160, and 200 mm. The sample geometries obtained from the experimental studies are given in Fig. 2. The stroke distance was used as 40 mm to reveal the parameter effect in all experiments. No damage was observed in the test samples at this stroke value.

Results and Discussion

After the experimental studies, firstly, the force-stroke curves of each experiment were obtained. Force data are obtained by the load cell of the test machine. In addition, for a better comparison, the bending moment-angle relation of sections can be calculated. Chen [34] presented the relation between force and bending moment can be converted by:

$$M = P.s/4 \tag{1}$$

$$\theta = 2\arctan\frac{2\delta}{s} \tag{2}$$

where P and δ are the force and displacement of the punch, M and Θ are the bending moment and rotation angle, respectively and at last, s represents the span between supports. Using Eq. (1) and Eq. (2) moment-angle curves of the samples are calculated. Force-Stroke and Moment-Angle curves are presented in Figs. 3, 4, 5, 6, 7 and 8.

When the force-stroke graphs were examined, it was observed that the force values decreased with increasing span distance in all cross-section forms. Again, it was determined that the force values increased as the punch radius increased in all sections. When the section geometries were examined at the same stroke value, the highest force values were observed in the square section and the lowest force values were observed in the tube section. When the moment-angle graphs are examined, it has been determined that the bending angle values decrease with increasing span distance in all section geometries, and the angle values do not change with increasing punch radius. When the results are analyzed in terms of the moment; the bending moment

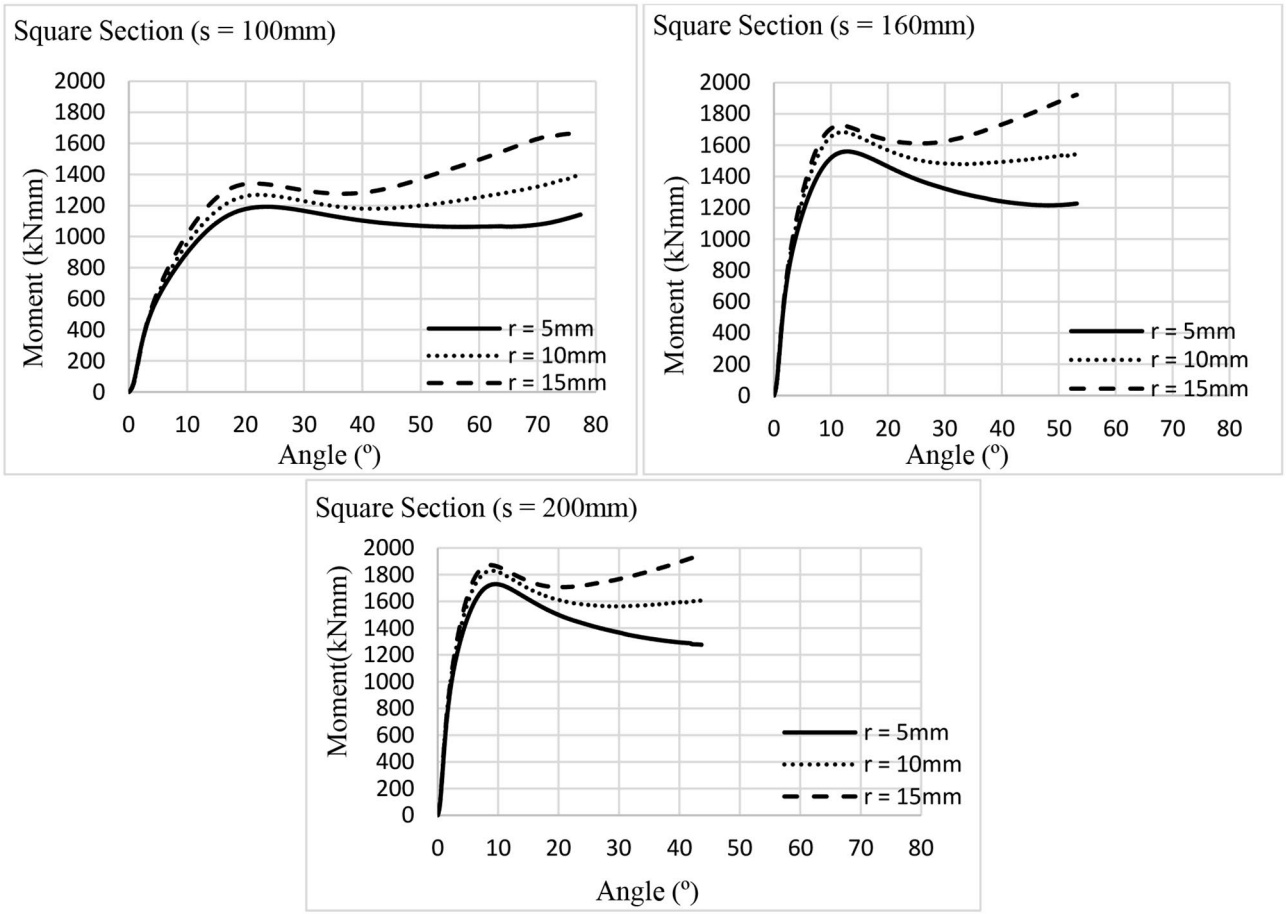

Fig. 4 Moment-Angle curves for square section with different punch radius

Fig. 5 Force-Stroke curves for rectangular section with different punch radius

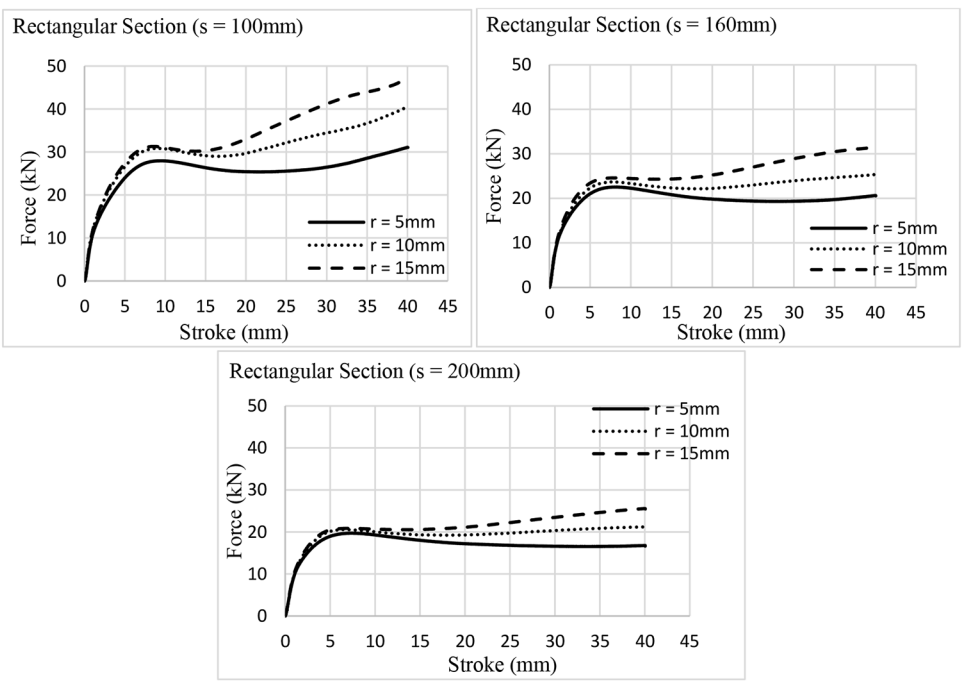

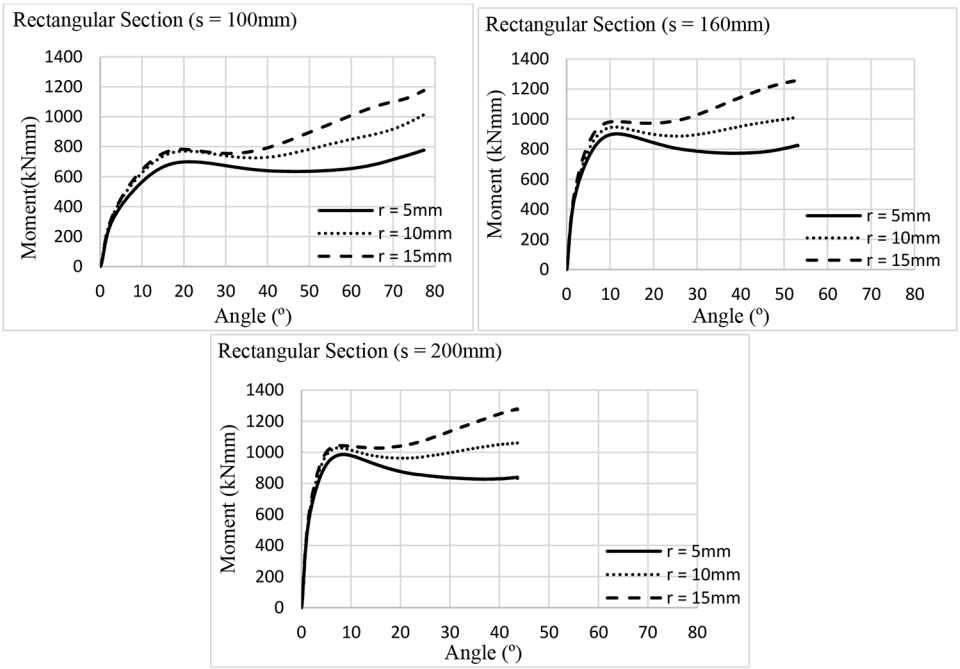

Fig. 6 Moment-Angle curves for rectangular section with different punch radius

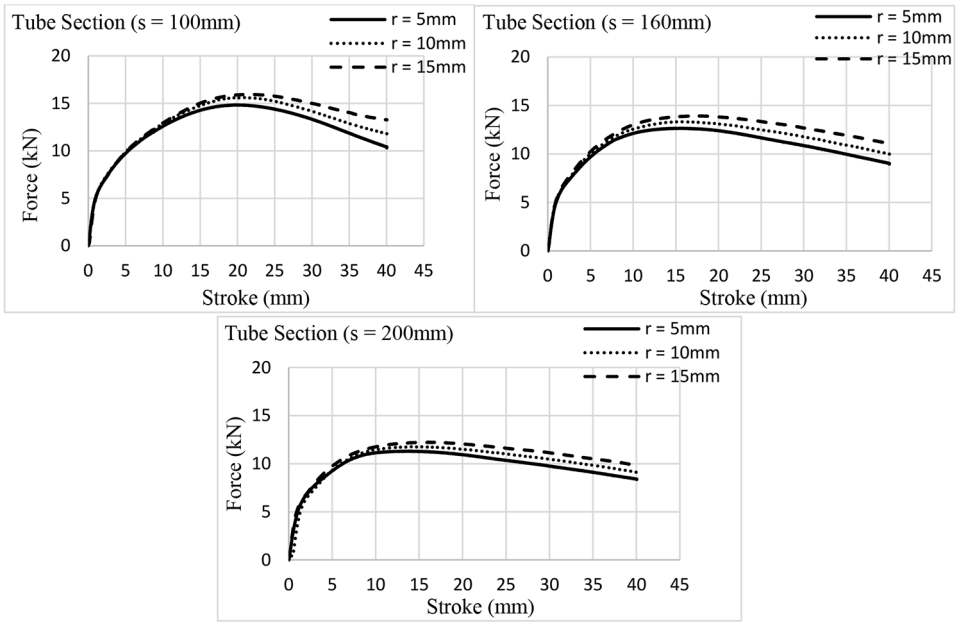

Fig. 7 Force-Stroke curves for tube section with different punch radius

of a structure basically depends on the force intensity and the effort distance (span distance in three-point bending). In tree-point bending, as the force intensity and span distance increase, the bending moment also increases. In this study, it is presented that the force intensity increases with increasing punch radius (Figs. 3 and 5, and Fig. 7). For these reasons, it can be concluded that the bending moment values increase with increasing span distance and increasing punch radius.

In the last step of the study, the energy absorption characteristics of the section geometries were obtained by using force-stroke graphs. The amount of energy absorbed during the three-point bending tests was determined by calculating the area values under the force-stroke curves for each

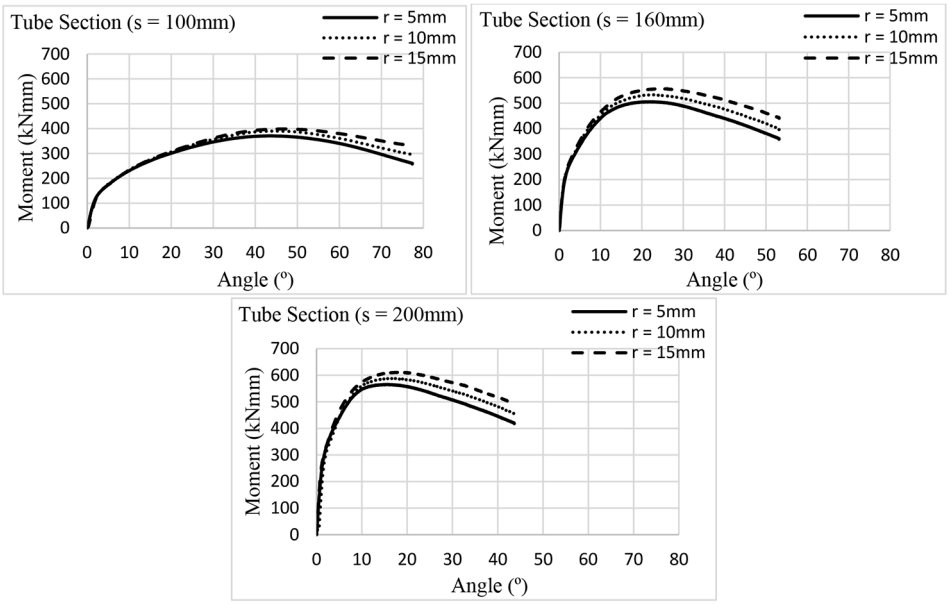

Fig. 8 Moment-Angle curves for tube section with different punch radius

Table 2 Absorbed energy values for s235 steel with different loading parameters

SECTION	Punch Radius (mm)	Span Distance (mm)	Energy (J)	Mean Force (kN)	Peak Force (kN)	Mean Bending Moment (kNmm)	Peak Bending Moment (kNmm)
SQUARE	5	100	1662.41	41.46	47.70	1036.45	1192.42
		160	1285.05	32.04	39.00	1281.76	1560.25
		200	1122.71	27.99	34.60	1399.27	1730.00
	10	100	1867.55	46.57	56.11	1164.27	1402.81
		160	1461.48	36.45	42.08	1457.90	1683.25
		200	1251.78	31.21	36.60	1560.71	1830.16
	15	100	2114.88	52.75	66.58	1318.80	1664.61
		160	1617.07	40.32	48.06	1612.96	1922.25
		200	1368.68	34.12	39.00	1705.92	1949.84
RECTANGULAR	5	100	1023.39	25.51	31.10	637.80	777.42
		160	787.76	19.64	22.56	785.53	902.50
		200	681.42	16.99	19.73	849.69	986.72
	10	100	1224.56	30.54	40.53	763.53	1013.20
		160	896.84	22.37	25.36	894.70	1014.25
		200	774.39	19.31	21.22	965.74	1061.09
	15	100	1364.13	34.02	47.02	850.58	1175.39
		160	1024.04	25.54	31.45	1021.46	1258.00
		200	853.96	21.29	25.58	1064.44	1279.22
TUBE	5	100	493.19	12.30	14.84	307.46	371.09
		160	431.28	10.75	12.64	430.16	505.75
		200	391.96	9.77	11.31	488.61	565.47
	10	100	518.66	12.93	15.61	323.23	390.31
		160	457.82	11.42	13.33	456.66	533.00
		200	408.67	10.19	11.77	509.60	588.59
	15	100	537.12	13.39	15.95	334.74	398.83
		160	484.26	12.07	13.93	482.97	557.25
		200	432.03	10.77	12.24	538.49	612.19

span distance and each punch radius of the materials in different section geometries. The obtained values are given in Table-2. As can be seen from the Table 2, it has been observed that as the amount of span distance increases, the absorbed energy decreases in all sections. However, it was determined that the energy absorbed increased with increasing punch radius values. When the results were examined in terms of section geometries, the highest energy values were calculated in the square section and the lowest energy values were calculated in the tube section.

Conclusion

In this study, the behavior of s235 structural steel under three-point bending was examined in three different section geometries as square, rectangular and, tube. Experimental studies were performed using three different punch geometries and three different span distances for each section. In this context, 100 mm, 160 mm, and 200 mm span distances and 5 mm, 10 mm, and 15 mm punch radius were used to exhibit loading parameter effects on bending and energy absorption behaviors of the s235 steel. For this reason, firstly, experimental studies were conducted and force-stroke curves for all loading parameters were obtained.

It was observed that the force values decreased with increasing span distance in all cross-section forms. Again, it was determined that the force values increased as the punch radius increased in all sections. Force-stroke curves show a similar behavior by means of section geometries. In square and rectangular sections, force values suddenly increase till approximately 8 mm stroke then force values decrease till 20 mm stroke, and at last, a slight increase is obtained till 40 mm stroke. In tube sections, force values increase till approximately 20 mm stroke and then decrease till 40 mm stroke. It is seen that tube profiles exhibit the lower force values with all loading parameters. The maximum force value for the tube section was obtained as 13.28 kN with a 5 mm punch radius and 100 mm span distance when square and rectangular sections present 66.56 kN and 47 kN maximum force values, respectively at the same loading conditions. Inertia moments of the sections have an important role in the bending process. Inertia moments of the sections used in this study are calculated as 75,100 mm^4, 52,620 mm^4, and 43,300 mm^4 for square, rectangular, and tube sections, respectively. It can be concluded that the force values increase with increasing inertia moments.

When it comes to the bending moment-angle behavior of the sections, it has been determined that the bending angle values decrease with increasing span distance in all section geometries, and the angle values do not change with increasing punch radius. When the results are analyzed in terms of the moment, it is observed that the bending moment values increase with increasing support spacing distance and increasing punch radius.

At last, energy absorption mechanisms are discussed in this study. It has been observed that as the amount of span distance increases, the absorbed energy decreases in all sections. However, it was determined that the energy absorbed increased with increasing punch radius values.

It can be concluded that the influence of section geometries of thin-walled structures, span distance, and punch radius has a significant effect on the deformation pattern and force/bending moment response of thin-walled structures. The dominant parameter is obtained as the span distance, while the punch radius has a lower influence on bending behavior when compared with the span distance.

Declarations

Conflict of Interest The authors declare that they have no known competing financial interests or personal relationships that could have appeared to influence the work reported in this paper.

References

1. Zhang J, Zhou H, Wu L, Chen G (2015) Bending Collapse Theory of Thin-Walled Twelve Right-Angle Section Beams Filled With Aluminum Foam. Thin-Walled Struct 94:45–55
2. Mo'tamedi M, Zeinoddini M, Elchalakani M (2018) A Closed-Form Analytical Solution for The Ratcheting Response of Steel Tubes With Wall-Thinning Under Inelastic Symmetric Constant Amplitude Cyclic Bending. Thin-Walled Struct 132:558–573
3. Yin H, Xiao Y, Wen G, Qing Q, Deng Y (2015) Multiobjective Optimization for Foam-Filled Multi-Cell Thin-Walled Structures Under Lateral Impact. Thin-Walled Struct 94:1–12
4. Qi C, Sun Y, Hu HT, Wang D-Z, Cao G-J, Yang S (2016) On Design of Hybrid Material Double-Hat Thin-Walled Beams Under Lateral Impact. Int J Mech Sci 118:21–35
5. Li Z, Zheng Z, Yu J, Guo L (2013) Crashworthiness of Foam-Filled Thin-Walled Circular Tubes Under Dynamic Bending. Mater Des 52:1058–1064
6. Hilditch T, Atwell D, Easton M, Barnett M (2009) Performance of Wrought Aluminium and Magnesium Alloy Tubes in Three-Point Bending. Mater Des 30:2316–2322
7. Duarte I, Vesenjak M, Krstulovic-Opara L (2014) Dynamic and Quasi-Static Bending Behaviour of Thin-Walled Aluminium Tubes Filled with Aluminium Foam. Compos Struct 109:48–56
8. Zhang Y, Xu X, Liu S, Chen T, Hu Z (2018) Crashworthiness Design for Bi-Graded Composite Circular Structures, Constr. Build Mater 168:633–649
9. Zhang X, Zhang H, Wang Z (2016) Bending Collapse of Square Tubes with Variable Thickness. Int J Mech Sci 106:107–116
10. Sun G, Tian X, Fang J, Xu F, Li G, Huang X (2015) Dynamical Bending Analysis and Optimization Design for Functionally Graded Thickness (FGT) Tube. Int J Impact Eng 78:128–137
11. Zhang X, Zhang H, Leng K (2018) Experimental and Numerical İnvestigation on Bending Collapse of Embedded Multi-Cell Tubes. Thin-Walled Struct 127:728–740
12. Zhang X, Zhang H, Ren W (2016) Bending Collapse of Folded Tubes. Int J Mech Sci 117:67–78

13. Xiao Z, Fang J, Sun G, Li Q (2015) Crashworthiness Design for Functionally Graded Foam-Filled Bumper Beam. Adv Eng Softw 85:81–95
14. Huang Z, Zhang X (2018) Three-Point Bending Collapse of Thin-Walled Rectangular Beams. Int J Mech Sci 144:461–479
15. Xiong Z, Hui Z (2018) Static And Dynamic Bending Collapse of Thin-Walled Square Beams with Tube Filler. Int J Impact Eng 112:165–179
16. Xiang XM, Lu G, Wang ZH (2015) Quasi-Static Bending Behavior of Sandwich Beams with Thin-Walled Tubes As Core. Int J Mech Sci 103:55–62
17. Wang J, Cheng X, Yan L, Wu C (2020) Numerical Study on I-Section Steel-Reinforced Concrete-Filled Steel Tubes (SRCFST) Under Bending. Eng Struct 225:111–276
18. Liu Q, Xu X, Ma J, Wang J, Shi Y, Hui D (2017) Lateral Crushing and Bending Responses of CFRP Square Tube Filled with Aluminum Honeycomb. Compos B Eng 118:104–115
19. Reyes A, Hopperstad OS, Hanssen AG, Langseth M (2004) Modeling of Material Failure in Foam-Based Components. Int J Impact Eng 30:805–834
20. Crupi V, Montanini R (2007) Aluminium Foam Sandwiches Collapse Modes Under Static and Dynamic Three-Point Bending. Int J Impact Eng 34:509–521
21. Fang J, Gao Y, Sun G, Zhang Y, Li Q (2014) Parametric Analysis and Multiobjective Optimization for Functionally Graded Foam-Filled Thin-Wall Tube Under Lateral Impact. Comput Mater Sci 90:265–275
22. Kim HT, Reid SR (2001) Bending Collapse of Thin-Walled Rectangular Section Columns. Comput Struct 79:1897–1911
23. Mamalis AG, Varvarigou TA, Litke AO, Manolakos DE, Loannidis MB, Kostazos PK, Andronikou VI, Karanastasis EA (2008) Bending of Cylindrical Steel Tubes: Numerical Simulation Using Grid Computing. Int J Crashworthiness 13(1):109–116
24. Mamalis AG, Manolakos DE, Loannidis MB, Kostazos PK (2006) Bending of cylindrical steel tubes: numerical modelling. Int J Crashworthiness 11(1):37–47
25. Kotelko M, Lim TH, Rhodes J (2000) Post-Failure Behaviour of Box Section Beams Under Pure Bending (An Experimental Study). Thin-Walled Struct 38:179–194
26. Zhang H, Sun G, Xiao Z, Li G, Li Q (2018) Bending Characteristics of Top-Hat Structures Through Tailor Rolled Blank (TRB) Process. Thin-Walled Struct 123:420–440
27. Wang Z, Li Z, Zhang X (2016) Bending Resistance of Thin-Walled Multi-Cell Square Tubes. Thin-Walled Struct 107:287–299
28. Zhu G, Wang Z, Cheng A, Li G (2017) Design Optimisation of Composite Bumper Beam With Variable Cross-Sections for Automotive Vehicle. Int J Crashworthiness 22(4):365–376
29. Chen D, Sun G, Jin X, Li Q (2020) Quasi-Static Bending and Transverse Crushing Behaviors for Hat-Shaped Composite Tubes Made of CFRP, GFRP and Their Hybrid Structures. Compos Struct 239:111842
30. Wang Z, Li Z, Xiong W (2019) Numerical Study on Three-Point Bending Behavior of Honeycomb Sandwich with Ceramic Tile. Compos B Eng 167:63–70
31. Huang Z, Zhang X, Fu X (2020) On The Bending Force Response of Thin-Walled Beams Under Transverse Loading. Thin-Walled Struct 154:106807
32. Solomon MM, Gerengi H, Kaya T, Kaya E, Umoren SA (2017) Synergistic inhibition of St37 steel corrosion in 15% H2SO4 solution by chitosan and iodide ion additives. Cellulose 24:931–950
33. Yazdani M, Toroghinejad MR, Hashemi SM (2015) Investigation of Microstructure and Mechanical Properties of St37 Steel-Ck60 Steel Joints by Explosive Cladding. J Mater Eng Perform 24(10):4032–4043
34. Chen W (2001) Experimental and numerical study on bending collapse of aluminum foam-filled hat profiles. Int J Solids Struct 38(44–45):7919–7944